Constituents of the Quasiparticle Spectrum Along the Nodal Direction of High-T_c Cuprates

A. A. Kordyuk,[1,2] S. V. Borisenko,[1] V. B. Zabolotnyy,[1] J. Geck,[1] M. Knupfer,[1] J. Fink,[1] B. Büchner,[1] C. T. Lin,[3] B. Keimer,[3] H. Berger,[4] A. V. Pan,[5] Seiki Komiya,[6] and Yoichi Ando[6]

[1]*Institut für Festkoerper und Werkstofforschung Dresden, Post Office Box 270116, D-01171 Dresden, Germany*
[2]*Institute of Metal Physics of National Academy of Sciences of Ukraine, 03142 Kyiv, Ukraine*
[3]*Max-Planck Institut für Festkörperforschung, 70569 Stuttgart, Germany*
[4]*Institut de Physique de la Matiére Complexe, Ecole Polytechnique Fédérale de Lausanne, 1015 Lausanne, Switzerland*
[5]*Institute for Superconducting and Electronic Materials, University of Wollongong, Wollongong, NSW 2522, Australia*
[6]*Central Research Institute of Electric Power Industry, Komae, Tokyo 201-8511, Japan*

(Received 27 October 2005; published 6 July 2006)

Applying the Kramers-Kronig consistent procedure, developed earlier, we investigate in detail the formation of the quasiparticle spectrum along the nodal direction of high-T_c cuprates. The heavily discussed "70 meV kink" on the renormalized dispersion exhibits a strong temperature and doping dependence when purified from structural effects such as bilayer splitting, diffraction replicas, etc. This dependence is well understood in terms of fermionic and bosonic constituents of the self-energy. The latter follows the evolution of the spin-fluctuation spectrum, emerging below some doping dependent temperature and sharpening below T_c, and is mainly responsible for the formation of the kink in question.

DOI: 10.1103/PhysRevLett.97.017002 PACS numbers: 74.25.Jb, 71.15.Mb, 74.72.Hs, 79.60.−i

The nodal direction is thought to be the simplest place in the Brillouin zone of high-T_c cuprates where electron renormalization effects can be most easily understood. However, since the discovery of an energy scale in the experimental dispersion [1–3], the so-called "70 meV kink", its origin remains a matter of extensive debate [4–14], which now has converged into a vital dilemma: phonon versus spin fluctuations [15]. Historically, the kink has been associated with a coupling to the magnetic resonance mode because of its energy and doping dependence [2], its seemingly smooth evolution into a spectral dip when moving to the antinodal region [3,4], and its temperature dependence (emerging below T_c) [5]. At the same time, the persistence of the effect above T_c reported by another group [2] was taken as an argument against the resonance mode scenario. Moreover, a visual "ubiquity" of the kink for a number of families of cuprates in a wide range of doping and temperature [6] and recently found similarity between a fine structure seen in dispersion to an expected phonon spectrum [8] have made a strong claim in favor of phonon scenario. However, we have also recently reported a careful investigation of the scattering rate kink [10], which is a simple consequence of the Kramers-Kronig (KK) relation between the real and imaginary parts of the electron self-energy [12]. The observed strong dependence of this kink on doping and temperature (xT dependence) questions seriously the phonon scenario. Moreover, the odd parity [13] and strong dependence on Zn impurities [14] of the nodal scattering form solid arguments for the magnetic scenario. Thus, from a number of arguments from both sides, it seems that studies on the nature of the nodal kink have brought us to a stalemate, and an evident way to resolve it is to turn from a qualitative consideration of the kink effect to its quantitative analysis to derive the parameters of the bosonic spectrum that will enable unambiguous identification of its origin.

Recently we have developed a KK-consistent procedure [12] which allows extraction of both the self-energy and the underlying bare dispersion from the photoemission data, and, thus, to place the kink problem into a quantitative domain. Subsequently, we have applied this self-

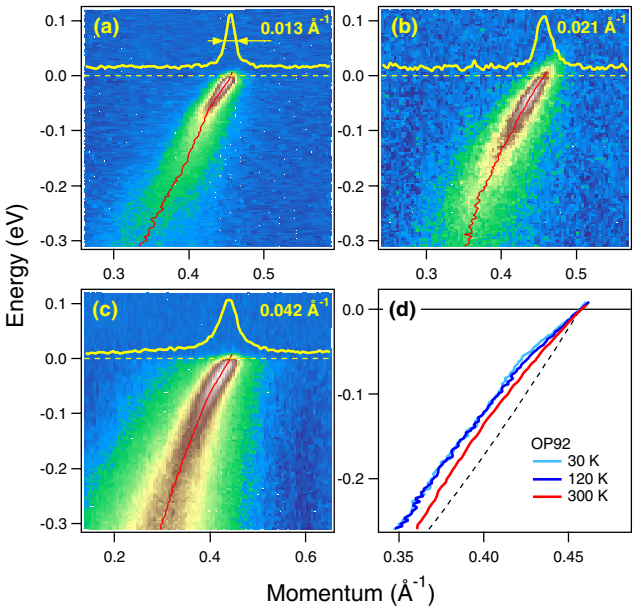

FIG. 1 (color online). Photoemission spectra for an optimally doped Bi-2212 measured at 30 K (a), and 120 K (b), and an overdoped LSCO measured at 40 K (c)—the yellow curves show MDCs at E_F; (d) some examples of experimental dispersions for OP Bi-2212 to illustrate a vanish of the kink with rising the temperature—the dashed line represents the bare dispersion.

consistent procedure to a number of nodal photoemission spectra measured at different temperatures and doping levels. Here we present the result of this investigation. We give a quantitative summary on the evolution of the nodal quasiparticle self-energy with doping and temperature and conclude a determinative role of the spin-fluctuations in this evolution.

We have analyzed the spectra from $Bi_2Sr_2CaCu_2O_{8+\delta}$: pure Bi-2212 and superstructure free Bi(Pb)-2212, and $La_{2-x}Sr_xCuO_4$ (LSCO) samples (we mark the samples according their doping and T_c). Some examples are shown in Figs. 1(a)–1(c). The self-consistency requirement sets rigorous constrains on the quality of the experimental data [12]. The widths of the E_F momentum distribution curves (MDC) are shown to illustrate the quality of the data we analyze. Under "quality" we imply here not only good experimental statistics and overall resolution but also a purity of spectra from artificial components, e.g., due to superstructure or sample inhomogeneities. Another complication comes from the finite bilayer splitting in Bi-2212 along the nodal direction [11]. Therefore, in order to pass the KK criterion, all the presented spectra of Bi-2212 have been measured with 27 eV photons, when the photoemission from the bonding band is highly suppressed [12].

Figure 1(d) is intended to illustrate a disappearance of the kink with rising temperature when the bonding band is suppressed: at 300 K only a hump on the dispersion remains. Comparing two "kinked" dispersions, it is clear that in order to get reliable information on the xT evolution of the kink-forming interactions, one should consider the difference of the data derived functions. This requires exceptional experimental statistics. All the mentioned constraints drastically decrease the amount of experimental data suitable for precise analysis.

Using the aforementioned procedure, which is thoroughly described in Ref. [12], the bare electron dispersion $\varepsilon(k)$ can be extracted from the photoemission intensity distributions similar to those shown in Figs. 1(a)–1(c). Consequently, both parts of the self-energy, $\Sigma'(\omega) = \omega - \varepsilon(k_m)$ and $\Sigma''(\omega) = [\varepsilon(k_1) - \varepsilon(k_2)]/2 \approx -v_F W$, are accessible as well. Here, for each ω, three momenta, $k_m(\omega)$, $k_1(\omega)$, and $k_2(\omega)$, are defined for the MDC $A(k)$ as $A(k_m) = \max[A(k)]$, $A(k_{1,2}) = \max[A(k)]/2$; the MDC width $2W = k_2 - k_1$; v_F is the bare Fermi velocity. In the following we focus on the self-energy functions derived from photoemission data.

The main results are summarized in Fig. 2(a) and 2(b) where we present the self-energy for the Bi-2212 samples of three doping levels: underdoped (UD77, $x = 0.11$), overdoped (OD75, $x = 0.20$), and optimally doped (OP92, $x = 0.16$). In Fig. 2(a) we plot $\Sigma'(\omega)$ for the underdoped and overdoped samples at different temperatures above T_c. The self-energies, almost identical at room temperature, become essentially different for lower temperatures (200 K and 120 K). In other words, an increase of $\Sigma'(\omega)$ with lowering the temperature is drastically different for overdoped and underdoped samples. However, in both

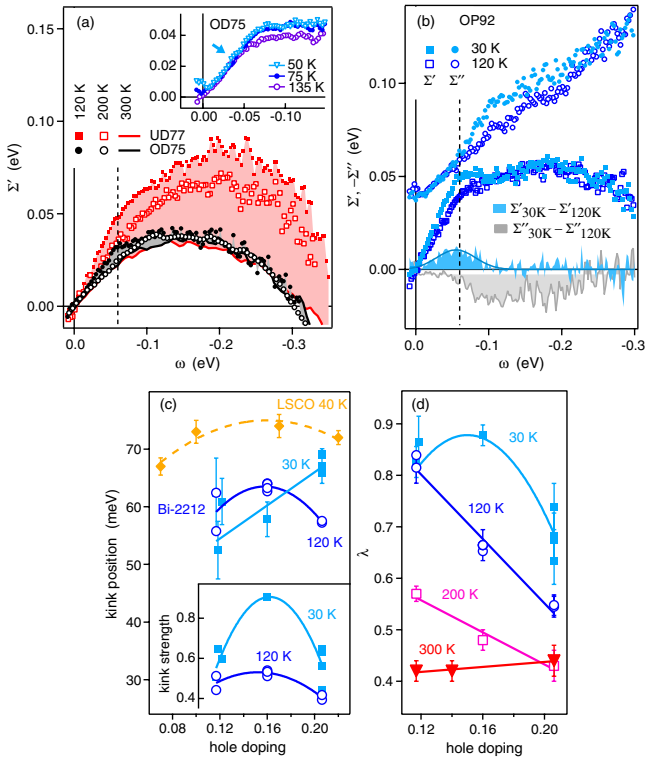

FIG. 2 (color online). (a), (b) Self-energy functions derived from experimental data for an overdoped, underdoped, and optimally doped Bi-2212 samples; the inset on (a) shows the data for OD75 taken ≈ 0.15 Å^{-1} away from the node to monitor the gap opening; on (b) the solid curve shows a fit of $\Sigma'(30\text{ K}) - \Sigma'(120\text{ K})$ to a Gaussian. (c), (d) The evolution of the kink parameters with hole concentration and temperature; different points correspond to different samples; the error bars are derived from a number of measurements of each sample.

cases, this increase exhibits a kink close to 60 meV (vertical dashed line).

The inset illustrates the persistence of the kink feature for the overdoped samples over the superconducting transition. Here we show $\Sigma'(\omega)$ extracted from the spectra taken ≈ 0.15 Å^{-1} away from the node to monitor the presence of the superconducting gap, which affects the MDC dispersion at low energy. The position of the kink remains unchanged over the superconducting transition but decreases with further increase of the temperature. Here one can notice some feature around 40 meV that appears with the gap opening. This should be a natural consequence of the gapped density of states and illustrates a rather weak effect of it on the nodal dispersion.

In Fig. 2(b), for an optimally doped sample, we examine the evolution of both $\Sigma'(\omega)$ and $\Sigma''(\omega)$, and compare the data taken at 30 K and 120 K. The shaded areas represent the change in the real and imaginary parts. While the increase in $\Sigma'(\omega)$ with lowering the temperature from 300 K to 120 K for the UD and OP samples are dramatic (the room temperature Σ' for OP92 is not shown but coincides with the corresponding curves for UD77 and OD75), in the range from 120 K to 30 K only a sharpening

of the kink is observed. Note that while the kink feature on $\Sigma'(\omega)$ at both temperatures stays approximately at the same energy, their difference is peaked at some lower energy ($\approx$50 meV; the solid curve shows its fit to a Gaussian) which is in agreement with an earlier result [5].

Following the tradition of model independent data treatment we fit the self-energy (in the energy range about 150 meV below E_F) to a simple kink function $-\Sigma'(\omega) = \lambda\omega(|\omega| < \omega_k) + (\lambda_h\omega + C)(|\omega| > \omega_k)$. The fitting parameters—kink position ω_k, kink strength $|\lambda - \lambda_h|$, and coupling strength λ—are plotted in Fig. 2(c) and 2(d) as function of doping and temperature.

The presented ω dependences of Σ' are consistent with the idea of two channels in the scattering process which was deduced earlier from the qualitative analysis of the scattering rate [10]. Owing to the results presented here the idea of two channel scattering is not only supported by more careful analysis but also, using the advantage of the KK-consistent procedure [12], can be described quantitatively. In the following interpretation we describe a model consistent with the experimental data.

We distinguish two scattering channels which we mark as "primary" and "secondary" (Σ_1 and Σ_2). The former is mainly xT independent while the latter exhibits a critical dependence on both temperature and doping.

In Fig. 2(a), the x independence of the *primary* channel is illustrated by almost identical $\Sigma'(\omega)$ at 300 K for the underdoped and overdoped samples, while the T independence is seen if one compares $\Sigma'(\omega)$ at 300 K and 200 K for the overdoped sample. Because of such xT independence and structureless energy dependence, the primary channel can be naturally associated with the direct electron-electron Coulomb interaction which results in an Auger-like scattering, the process when a hole decays into two holes and one electron [10]. In close vicinity to the Fermi level, this process forms the quasiparticles of the Fermi liquid type with $\Sigma_1' = -\lambda\omega$, $\Sigma_1'' \propto \omega^2 + (\pi T)^2$. In a finite energy range, the self-energy depends on the quasiparticle density of states (DOS), following the asymptotic behavior until DOS(ω) = const. On a large scale, a confined DOS (with a cutoff at $\sim\omega_c$) leads to a nonmonotonic $\Sigma_1''(\omega)$—roughly, it reaches a maximum at ω_c. Being KK related, $\Sigma_1'(\omega)$ reaches its maximum close to an inflexion point of $\Sigma_1''(\omega)$ and at ω_c goes to zero. This behavior is schematically shown in Fig. 3 by the dashed lines. Here we should note that the deduced value $\omega_c \approx 0.3$ eV is approximately 3 times smaller than the bare band width ω_0 [12], which is difficult to explain by simple renormalization of the bare DOS. A possible explanation can be related with the highly nonuniform real DOS due to the van Hove singularities caused by the saddle points and/or with kinematic constraints. The latter seems to be really essential if we recall a very small effect of the gap opening on low energy part of $\Sigma'(\omega)$ [see the inset in Fig. 2(a)]; so one can conclude that the effective DOS, which forms the self-energy of nodal quasiparticles, consists of states mainly from the nodal

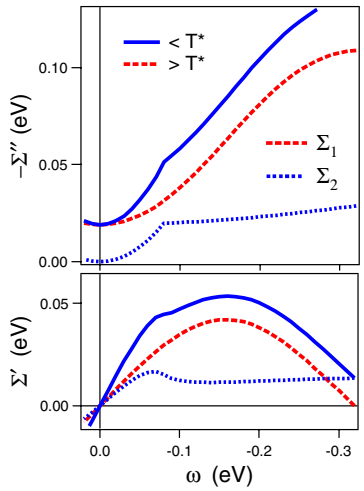

FIG. 3 (color online). Schematic summary of the temperature evolution of the real (bottom) and imaginary (top) parts of the self-energy based on the data for the optimally doped sample.

region. Thus, except the temperature dependent offset of the scattering rate, $\Sigma''(0, T)$, the temperature and doping dependence of the primary scattering channel appears only through the effective DOS and remains weak. This channel can be mainly described by two xT-independent parameters, a coupling strength $\lambda_1 = 0.43 \pm 0.02$ and scattering cutoff $\omega_{c1} = 0.35 \pm 0.05$ eV.

The *secondary* channel is essentially different. First, it exhibits very different behavior—it gradually appears only below some temperature, while both this temperature and strength of the channel are progressively increasing with underdoping. Second, the channel is not structureless but reveals some energy scale that implies a certain structure of the interactions involved. It is this structure that forms the 70 meV kink, depending on doping [Fig. 2(c)] and changing over the superconducting transition [Fig. 2(b)].

The shape of $\Sigma_2''(\omega)$ (see Fig. 3) indicates a bosonic origin of the secondary scattering channel, a process during which a hole decays into another hole and a bosonic excitation. In the simplest case of constant electronic DOS the coupling to a single bosonic mode would result in a steplike function. In the general case, $\Sigma_2''(\omega)$ is a cross correlation of the bosonic and electronic density of states. Therefore, a careful examination of this channel will not only reveal the origin of relevant bosons but also provide parameters of the bosonic spectrum which can help to understand the nature of superconducting coupling. Phonons and spin-fluctuations are considered as the most probable candidates for the role of the main scattering bosons [15]. In the following we discuss which of them can be consistent with the experimental data, and, since it is not necessary that the secondary channel is formed by bosons of only one type, we split the problem into two parts. (1) We derive the properties of the bosonic spectrum which makes a global contribution into secondary channel. (2) We discuss the structure of the scattering rate and

whether it is possible to identify it with bosons of a certain type.

The global contribution to $\Sigma_2(\omega)$ can be evaluated in terms of a coupling strength of this channel $\lambda_2 = \lambda - \lambda_1$. The strong dependence of this parameter on temperature and doping can be seen in Fig. 2(d): being negligible at room temperature it grows as big as λ_1 at low temperatures (for UD and OP) and, e.g., at 120 K, it grows from 0.1 to 0.4 when the hole concentration is decreasing from $x = 0.21$ (OD75) to 0.12 (UD77). At temperatures higher than T_c, λ_2 exhibits monotonic dependence on doping. We believe that λ_2 vanishes at $T^*(x)$, which is consistent with the previous qualitative consideration [10], although from current results we can only deduce that $T^*(0.21) < 200\ \mathrm{K} < T^*(0.16)$. The 70 meV kink behaves similarly, or, at least, it vanishes together with λ_2. This leads us to believe that the kink is an inherent feature of a bosonic spectrum which makes the main contribution to $\Sigma_2(\omega)$.

Common sense suggests that phonons cannot be responsible for such a dramatic doping and temperature dependence of the channel strength. Only softening of some bosonic modes has been reported (e.g., see Ref. [16]) but it seems unlikely that the phononic spectrum can completely disappear with doping or temperature. One can get an additional argument from *purified* $\Sigma_2''(\omega)$ (see Fig. 3) that does not saturate up to 300 meV binding energy, which is difficult to reconcile with a ~90 meV confined phononic spectrum [16]. On the other hand, the shape of $\Sigma_2''(\omega)$ is reminiscent of the spin-fluctuation scattering (continuum plus mode) [17], although the energy of the scattering kink in experiment is notably higher: 100 meV [10] instead of 70 meV [17]. From this "energy argument", a more general assumption that the 100 meV energy scale in scattering, which results in the 70 meV kink in dispersion, is formed by the gaped continuum [18] seems more adequate. Moreover, a recently predicted new mode in spin susceptibility [19] seems to fit the presented data very well. Therefore we may conclude here that the secondary channel in the nodal scattering is mainly caused by an indirect interaction between electrons through the spin-fluctuations.

Remarkably, the $\omega_k(x)$ dependences above and below T_c are qualitatively different: Above T_c [Fig. 2(c), 120 K for BSCCO and 40 K for LSCO], $\omega_k(x)$ is nonmonotonic with a maximum about optimal doping level. Below T_c, it becomes monotonic, which is in agreement with earlier results for BSCCO [20] and recent results for YBCO [21]. Such a dramatic evolution of $\omega_k(x)$ [as well as of $\lambda_2(x)$; see Fig. 2(d)] over the superconducting transition suggests a mutual renormalization of electronic and bosonic spectra, while the nonmonotonic dependences of the kink strength and λ on x suggest a relationship of the spin-fluctuations to the mechanism of high-T_c superconductivity.

Finally, it can happen that the situation is more complex than it is seen. Phonons might make an observable contribution to the kink story, interfering with the spin-fluctuation kink in its dependence on doping and over the superconducting transition. In this case, however, the maximum coupling to the phonons can be estimated as $\lambda_{\mathrm{ph}} \sim 0.1$, which practically rules them out as a glue for the superconducting pairing. Nevertheless it seems highly important to keep going in this direction improving the quality of the experimental data to be able to compare the bosonic spectrum extracted from photoemission to spectra of spin-fluctuations and phonons in order to find out the details of the pairing process.

In conclusion, we distinguish two principal channels of interactions which form the quasiparticle self-energy along the nodal direction of high-T_c cuprates. Both originate from interactions in the electronic subsystem, but while the primary channel is structureless and mainly xT independent and, therefore, can be naturally explained by a direct electron-electron scattering (the Auger process), the secondary channel exhibits a critical dependence on doping and temperature in agreement with the spin-fluctuation spectrum and can be explained by an indirect process via the magnetic degree of freedom. While the maximum of the renormalization is related with saturation of the Auger process, the kink feature on the dispersion appears only with underdoping and/or lowering temperature and is caused by an energy scale in the spin-fluctuation spectrum.

The project is part of the Forschergruppe FOR538. The work in Lausanne was supported by the Swiss National Science Foundation and by the MaNEP.

[1] T. Valla *et al.*, Science **285**, 2110 (1999).
[2] P. V. Bogdanov *et al.*, Phys. Rev. Lett. **85**, 2581 (2000).
[3] A. Kaminski *et al.*, Phys. Rev. Lett. **86**, 1070 (2001).
[4] M. Eschrig and M. R. Norman, Phys. Rev. Lett. **85**, 3261 (2000).
[5] P. D. Johnson *et al.*, Phys. Rev. Lett. **87**, 177007 (2001).
[6] A. Lanzara *et al.*, Nature (London) **412**, 510 (2001).
[7] X. J. Zhou *et al.*, Nature (London) **423**, 398 (2003).
[8] X. J. Zhou *et al.*, Phys. Rev. Lett. **95**, 117001 (2005).
[9] A. Koitzsch *et al.*, Phys. Rev. B **69**, 140507(R) (2004).
[10] A. A. Kordyuk *et al.*, Phys. Rev. Lett. **92**, 257006 (2004).
[11] A. A. Kordyuk *et al.*, Phys. Rev. B **70**, 214525 (2004).
[12] A. A. Kordyuk *et al.*, Phys. Rev. B **71**, 214513 (2005); A. A. Kordyuk and S. V. Borisenko, cond-mat/0510421.
[13] S. V. Borisenko *et al.*, Phys. Rev. Lett. **96**, 067001 (2006).
[14] V. B. Zabolotnyy *et al.*, Phys. Rev. Lett. **96**, 037003 (2006).
[15] A. Damascelli, Z. Hussain, and Z.-X. Shen, Rev. Mod. Phys. **75**, 473 (2003).
[16] R. J. McQueeney *et al.*, Phys. Rev. Lett. **87**, 077001 (2001).
[17] M. Eschrig and M. R. Norman, Phys. Rev. B **67**, 144503 (2003).
[18] A. V. Chubukov and M. R. Norman, Phys. Rev. B **70**, 174505 (2004).
[19] I. Eremin *et al.*, Phys. Rev. Lett. **94**, 147001 (2005).
[20] A. D. Gromko *et al.*, Phys. Rev. B **68**, 174520 (2003).
[21] S. V. Borisenko *et al.*, Phys. Rev. Lett. **96**, 117004 (2006).